# Ultrafast Excited-State Dynamics of Oxazole Yellow DNA Intercalators

Fürstenberg, Alexandre; Vauthey, Eric

# Ultrafast Excited-State Dynamics of Oxazole Yellow DNA Intercalators

**Alexandre Fürstenberg and Eric Vauthey***

*Department of Physical Chemistry of the University of Geneva, 30 quai Ernest-Ansermet, CH-1211 Geneva 4, Switzerland*

*Received: April 25, 2007; In Final Form: August 17, 2007*

The excited-state dynamics of the DNA intercalator YO-PRO-1 and of three derivatives has been investigated in water and in DNA using ultrafast fluorescence spectroscopy. In the free form, the singly charged dyes exist both as monomers and as H-dimers, while the doubly charged dyes exist predominantly as monomers. Both forms are very weakly fluorescent: the monomers because of ultrafast nonradiative deactivation, with a time constant on the order of 3−4 ps, associated with large amplitude motion around the methine bridge, and the H-dimers because of excitonic interaction. Upon intercalation into DNA, large amplitude motion is inhibited, H-dimers are disrupted, and the molecules become highly fluorescent. The early fluorescence dynamics of these dyes in DNA exhibits substantial differences compared with that measured with their homodimeric YOYO analogues, which are ascribed to dissimilarities in their local environment. Finally, the decay of the fluorescence polarization anisotropy reveals ultrafast hopping of the excitation energy between the intercalated dyes. In one case, a marked change of the depolarization dynamics upon increasing the dye concentration is observed and explained in terms of a different binding mode.

## Introduction

The synthesis of the YOYO and TOTO dye families has been a major breakthrough in the development of fluorescent DNA probes for molecular biology.[1,2] Indeed, they allowed for the first time DNA detection with sensitivity comparable to that of radioactive probes.[3] These dyes are homodimers of oxazole yellow (YO or YO-PRO-1) and thiazole orange (TO or TO-PRO-1), which are asymmetric cyanine dyes with a monomethine bridge connecting a benzo-1,3-oxazole and a benzo-1,2-thiazole moiety, respectively, to a quinoline group. Like many other cyanines, both dimeric (YOYO, TOTO) and monomeric (YO, TO) dyes have been shown to have two binding modes to DNA: (1) intercalation between adjacent base pairs, bisintercalation for the dimers, and (2) minor groove binding.[4−6] The first mode is dominant at high base pair to dye (bp/dye) ratio, that is, when the dye concentration is relatively low compared with that of DNA, while the second is favored at low bp/dye ratio.[5]

The ability of these dyes to operate as DNA probes comes from the fact that they are essentially nonfluorescent when free in aqueous solutions but highly fluorescent when bound to DNA. This huge enhancement of the fluorescence quantum yield upon binding to DNA was assumed to originate from the loss of mobility around the methine bridge due to the constrictive DNA environment.[7,8] In the free form, the excited dyes can undergo ultrafast nonradiative deactivation through large amplitude motion around this bridge. On the other hand, this nonradiative deactivation pathway is no longer operative in DNA where this motion is hindered.

We have recently shown that the fluorescence enhancement of YOYO derivatives upon DNA binding is only partially due to this mechanism.[9−11] Indeed, when free in water, these homodimeric dyes tend to form intramolecular H-type dimers. As a result of a strong excitonic interaction within these aggregates, the radiative transition from the lowest electronic excited state is characterized by a very small oscillator strength, and thus self-aggregated H-dimers are essentially nonfluorescent. This aggregation is disrupted upon bisintercalation into DNA, and because large amplitude motion is also hindered, fluorescence becomes the major deactivation pathway of the excited dyes. The decrease of excitonic coupling between the YO moieties upon intercalation into DNA is not so much due to a larger interchromophoric distance as to the angle between them of ca. 83° imposed by the natural pitch of the DNA helix. Under these conditions, excitation is localized on a single chromophoric unit but can hop from one moiety to another within a few picoseconds as revealed by fluorescence polarization anisotropy measurements.

As a result of the coexistence of aggregated and nonaggregated forms, the fluorescence decay of YOYO dyes in water exhibits an ultrafast decay with a time constant on the order of 4 ps, due to the nonaggregated dyes undergoing large amplitude motion around the monomethine bridge, and additionally a very small decay component with a much larger time constant due to the self-aggregated dimers.

Spectral dynamics with a ∼1 ps time constant corresponding to dynamic Stokes shift was also observed with YOYO dyes both free in water and bound to DNA. This feature was ascribed to solvent relaxation through diffusive motion of the water molecules, the smaller amplitude of this component in DNA being in agreement with a smaller exposure of the intercalated chromophores to water. This result revealed that these dyes could also be used to probe the environmental dynamics in DNA.

We report here on a detailed study of the excited-state dynamics of monomeric fluorescent DNA probes of the YO family both free in aqueous solutions and bound to DNA using time-resolved fluorescence spectroscopy. The main motivation was to obtain a more complete picture of the effect of DNA binding on the excited-state properties of these widely used

* Corresponding author. E-mail: eric.vauthey@chiphy.unige.ch.

10.1021/jp073182t CCC: $37.00 
Published on Web 10/11/2007

**SCHEME 1**

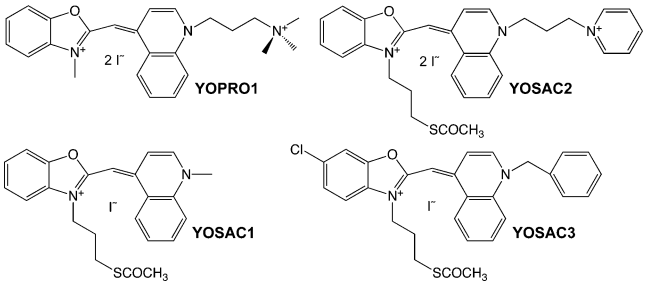


DNA probes. To our knowledge, no information on the ultrafast excited-state dynamics of these monomeric dyes in water and in DNA is available in literature.

The investigated dyes are the commercial YO-PRO-1 and its three analogues, YOSAC1 to YOSAC3 (Scheme 1). Although they all have a rather similar structure, they differ by their electric charge, two of them being singly charged (YOSAC1 and YOSAC3) and the two others being doubly charged (YO-PRO-1 and YOSAC2). We will show that, while this difference has a major impact on the aggregation in water and binding to DNA, it has no significant influence on their excited-state properties. However, differences between YO and YOYO dyes exist when their ultrafast dynamics in DNA is considered.

## Experimental Section

**Samples.** The dyes were provided by Professor T. Deligeorgiev (Faculty of Chemistry, University of Sofia) and were used as received. Their synthesis has been reported in ref 12. Methanol (MeOH) and decanol (DeOH) were from Acros Organics, ethanol (EtOH) and DMSO from Fluka, butanol (BuOH) from Merck, phosphate-buffered saline (PBS, composition NaCl 137 mM, KCl 26.8 mM, $Na_2HPO_4$ 8.1 mM, $KH_2PO_4$ 1.5 mM) and double-stranded salmon sperm DNA from Sigma, and ethylenediaminetetraacetic acid (EDTA) disodium salt dihydrate from AppliChem. All compounds were of the highest commercially available grade and used without further purification. The absence of impurities in the solvents was checked by exciting the pure solvents at 400 nm and looking for any emission not attributable to Raman scattering. Stock solutions (2 mM) of the DNA-binding dyes in DMSO were prepared and stored in the dark. DNA (1 mg/mL) stock solutions in bidistilled water were stored at −20 °C. All samples were freshly prepared from the stock solutions. For steady-state and time-correlated single photon counting measurements, the dye concentration was on the order of 2−4 $\mu$M, and for fluorescence up-conversion experiments, it amounted to 200 $\mu$M. Unless specified, the experiments were performed in PBS containing 1 mM EDTA, except with YOSAC3, which was handled in distilled water to avoid J-aggregate formation, and the measurements with the bound dyes were performed with a DNA bp/dye ratio of 50. An average extinction coefficient of 13 200 $cm^{-1}\cdot M^{-1}$ per base pair was used to determine DNA concentrations.[13] All experiments were performed at 20 ± 2 °C.

**Steady-State Measurements.** Absorption spectra were recorded on a Cary 50 spectrophotometer, while fluorescence and excitation spectra were measured on a Cary Eclipse fluorimeter (5 nm slit) in a 1 cm quartz cell. Fluorescence spectra were recorded upon excitation at 440 nm and corrected for the wavelength-dependent sensitivity of the detection. Quantum yield measurements were performed against fluorescein in NaOH at pH 13 ($\Phi_{fl} = 0.95$)[14] or free YOYO-1 ($\Phi_{fl} = 0.0011$).[8] The relative error on the quantum yields is estimated to ±10%.

**Time-Resolved Fluorescence Measurements.** Excited-state lifetime measurements in the nanosecond time scale were carried out with the time-correlated single photon counting (TCSPC) technique as described earlier.[9] Excitation was performed at a repetition rate of 10 MHz with ∼60 ps pulses generated with a laser diode at 395 nm (Picoquant model LDH-P-C-400B). The full width at half-maximum (FWHM) of the instrument response function (IRF) was around 200 ps. The accuracy on the lifetimes is of ca. 0.1 ns.

Excited-state lifetime measurements on shorter time scales were performed using fluorescence up-conversion (FU). The experimental setup has been described in detail elsewhere.[15] Excitation was achieved at 400 nm with the frequency-doubled output of a Kerr lens mode-locked Ti:sapphire laser (Tsunami, Spectra-Physics). The output pulses centered at 800 nm had a duration of 100 fs and a repetition rate of 82 MHz. The polarization of the pump beam was at magic angle relative to that of the gate pulses at 800 nm except for fluorescence anisotropy measurements. Experiments were carried out in a 1 mm rotating cell. The FWHM of the IRF was ca. 280 fs.

Femtosecond-resolved fluorescence anisotropy measurements were carried out with the FU setup by changing the polarization of the pump beam with respect to the gate beam with a half-wave plate. The anisotropy decay, $r(t)$, was reconstructed using the standard equation, $r(t) = I_{||}(t) - I_{\perp}(t)/(I_{||}(t) + 2I_{\perp}(t))$, where $I_{||}(t)$ and $I_{\perp}(t)$ are the fluorescence intensities recorded with the polarization of the pump beam set parallel and perpendicular to that of the gate beam, respectively.

No significant degradation of the samples was observed after the measurements.

**Fluorescence Data Analysis.** The observed fluorescence time profile, $D(\lambda,t)$, could be reproduced by the convolution of the Gaussian-shaped IRF with a trial function, which, in our case, was a sum of one Gaussian and several exponential terms. The convolution of a Gaussian function (IRF) with another Gaussian function, $D_{I\otimes G}(\lambda,t)$, or with an exponential function, $D_{I\otimes E}(\lambda,t)$,[16] leads respectively to the following analytical expressions:

$$D_{I\otimes G}(\lambda,t) = \frac{a_1(\lambda)}{2\sqrt{1 + w^2/{\tau_1}^2}} \exp\left(\frac{(t-t_0)/\tau_1}{\sqrt{1 + w^2/{\tau_1}^2}}\right)^2 \left[1 + \mathrm{erf}\left(\frac{t-t_0}{w\sqrt{1 + w^2/{\tau_1}^2}}\right)\right] \quad (1a)$$

$$D_{I\otimes E,i}(\lambda,t) = \frac{a_i(\lambda)}{2} \exp\left(-\frac{t-t_0}{\tau_i}\right) \exp\left(-\frac{w^2}{4{\tau_i}^2}\right) \left[1 + \mathrm{erf}\left(\frac{t - t_0 - w^2/(2\tau_i)}{w}\right)\right] \quad (1b)$$

$$D(\lambda,t) = D_{I\otimes G}(\lambda,t) + \sum_{i=2}^{n} D_{I\otimes E,i}(\lambda,t) \quad (1c)$$

where $t_0$ is the center, $w$ is the Gaussian width of the IRF, $a_i$ and $\tau_i$ are the amplitude and time constant of the $i$th exponential function, and $a_1$ and $\tau_1$ are the amplitude and the inverse of the width of the Gaussian function. The normalized FU data were globally analyzed by adjusting an adequate sum of such terms, eq 1c, to the measured data points using a nonlinear least-squares fitting procedure (MATLAB, The MathWorks, Inc.). This approach is much faster than iterative numerical reconvolution and allows data sets with nonuniform spacing of the data points on the time axis to be dealt with. Measurements were carried

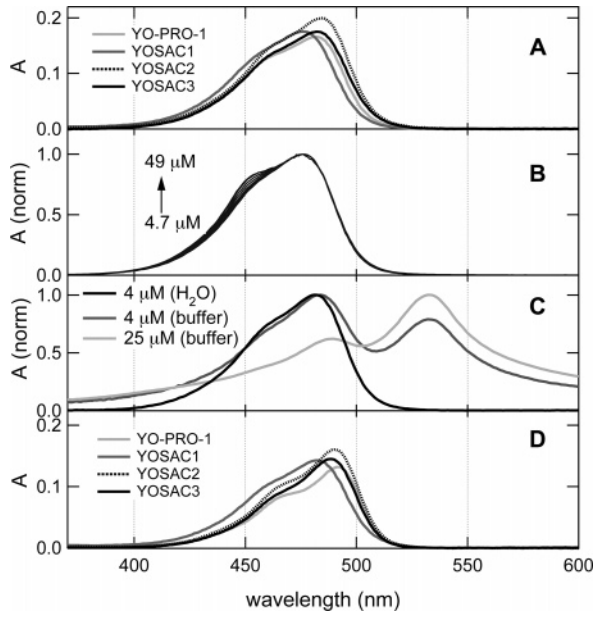


**Figure 1.** (A) Absorption spectra of 2 $\mu$M solutions of the dyes in water, (B) concentration dependence of the absorption spectrum of YOSAC2, (C) ionic strength dependence of the absorption spectrum of YOSAC3, and (D) absorption spectra of 2 $\mu$M solutions of the dyes with DNA (bp/dye ratio 50).

out at 8−9 detection wavelengths from 480 to 630 nm over time scales accurately covering the span of the fluorescence decay.

Once the global lifetimes were extracted with this procedure, the amplitudes of the different decay components were determined by rescaling the time profiles $D(\lambda,t)$ with the factor $F(\lambda)$:

$$F(\lambda) = \frac{S(\lambda)}{\int_0^\infty D(\lambda,t)\,\mathrm{d}t} \qquad (2)$$

where $S(\lambda)$ is the corrected steady-state fluorescence intensity.[17,18] To draw the decay-associated amplitude spectra, the sum of the positive amplitudes was set equal to 1 at 495 nm (maximum intensity in the spectrum). Time-resolved emission spectra were reconstructed from the analytical expressions obtained for the decays from the fitting procedure. The accuracy on the lifetimes and on the amplitudes obtained with this method is estimated to ca. 10%, except on lifetimes shorter than about 500 fs where the uncertainty is about 100 fs.

## Results

**Steady-State Spectra and Nanosecond Fluorescence Dynamics.** The absorption spectrum of all investigated dyes in the visible region consists of a single band centered between 475 and 485 nm (Figure 1A). For the singly charged YOSAC1 and YOSAC3, the relative absorbance at the blue side of the band increases with concentration, the absorption spectrum of YOSAC1 at high concentration exhibiting a growing shoulder around 450 nm (Figure 1B). Such concentration dependence is totally absent in organic solvents. This effect, which was not observed with the doubly charged dyes, YO-PRO-1 and YOSAC2, can be ascribed to the formation of H-type dimers. In these aggregates, the chromophores are arranged in face-to-face conformation with the transition dipole moments in parallel.[19] The blue shift of the absorption band upon aggregation is due to excitonic interaction. In H-dimers and in higher H-aggregates, the transition to the lowest excitonic state is essentially forbidden, while that to the upper excitonic state bears the whole oscillator strength. From the spectral shift, an excitonic coupling energy on the order of 1050 cm$^{-1}$, hence a ~2100 cm$^{-1}$ Davydov splitting, can be estimated for both YOSAC1 and YOSAC3. Similar blue shifts and thus coupling energies have been reported for the intramolecular H-dimer formed by YOYO-1[9] and for other cyanine H-dimers in water.[20] The absorption spectra remain unchanged in aqueous buffer solutions except for YOSAC3, whose spectrum changes dramatically upon addition of salt. As shown in Figure 1C, an additional band centered at 532 nm, whose relative intensity increases with dye concentration, appears in the absorption spectrum of YOSAC3 in buffer solutions. This new band can be ascribed to a J-aggregate, which is characterized by a head-to-tail arrangement of the chromophores.[19,21,22] Upon excitonic interaction, all the oscillator strength is concentrated in the transition to the lowest excitonic state, hence the red shift upon aggregation. From this shift, an excitonic coupling energy of ca. 1950 cm$^{-1}$ is deduced. Such J-aggregation was only observed with YOSAC3, which is the only dye to have a chlorine substituent. The presence of chlorine atoms on cyanines has been shown to facilitate the formation of J-aggregates.[23]

**TABLE 1: Fluorescence Quantum Yield of the Dyes (1−2 $\mu$M Concentration) Free in Water and with DNA (bp/dye Ratio 50)**

| dye | environment | $\Phi_{fl}$ |
|---|---|---|
| YO-PRO-1 | $H_2O$ | $2.4 \times 10^{-4}$ |
| | DNA | 0.42 |
| YOSAC1 | $H_2O$ | $5.3 \times 10^{-4}$ |
| | DNA | 0.35 |
| YOSAC2 | $H_2O$ | $3.6 \times 10^{-4}$ |
| | DNA | 0.41 |
| YOSAC3 | $H_2O$ | $9.7 \times 10^{-4}$ |
| | DNA | 0.61 |

Upon addition of DNA, the spectrum of all dyes shifts slightly to the red ($\Delta\bar{\nu} \approx -200$ cm$^{-1}$) and displays about 20% hypochromism (Figure 1D). A similar effect has been observed with YOYO derivatives and TO upon intercalation into DNA.[5,9,24] The shoulder at the blue side of the band can be ascribed to a vibronic transition.[7] In the case of YOSAC3, addition of DNA cannot totally suppress the J-aggregate band, indicating that the free energy gain upon intercalation into DNA is most probably not largely different from that associated with J-aggregation.

The fluorescence quantum yields, $\Phi_{fl}$, of the free dyes in water are very small (Table 1), in agreement with the occurrence of an ultrafast nonradiative deactivation of the excited state via large amplitude motion around the monomethine bridge. However, Table 1 reveals that, although very small, the fluorescence quantum yields of the singly charged dyes (YOSAC1 and YOSAC3) are higher than those of the doubly charged dyes. Moreover, Figure 2A indicates that the fluorescence spectra of the free dyes differ substantially. The spectra of the singly charged dyes are broad and almost structureless, while those of the doubly charged dyes are more structured and resemble more the mirror image of the corresponding absorption band. These differences can be ascribed to the propensity of singly charged dyes to aggregate.[11] These fluorescence spectra can be considered as being due to two emitting species: nonaggregated dyes with a very short fluorescence lifetime and a spectrum that should be essentially mirror image of the absorption spectrum and H-dimers with a longer lifetime but with a small radiative rate constant due to the excitonic coupling and a broad, red-shifted fluorescence spectrum as observed with YOYO dyes in water.[9] The fluorescence spectra of YO-PRO-1 and YOSAC2 are dominated by the emission from the nonaggregated dyes.

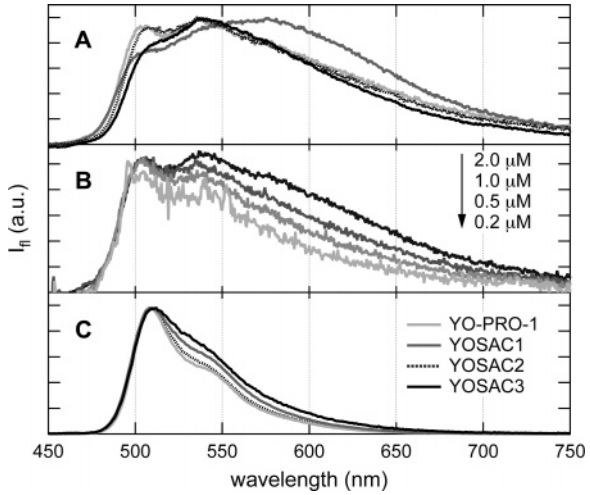


**Figure 2.** (A) Fluorescence spectra of the dyes in water (refer to legend in panel C), (B) concentration dependence of the fluorescence spectrum of YO-PRO-1 in water, and (C) fluorescence spectra of the dyes with DNA (bp/dye ratio 50).

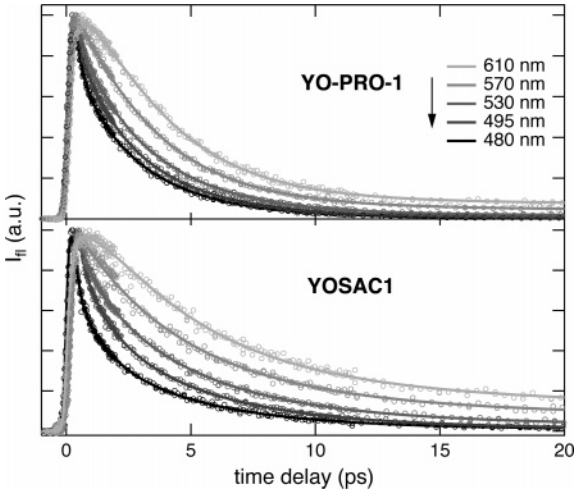


**Figure 3.** Wavelength dependence of the fluorescence dynamics of YO-PRO-1 and YOSAC1 in water.

The bands are however substantially broader than the mirror image of the absorption band indicating the presence of some H-dimers. This is supported by the narrowing of the fluorescence spectrum of YO-PRO-1 observed upon decreasing dye concentration (Figure 2B). At the lowest concentration measured, the fluorescence spectrum is very noisy but resembles rather closely the mirror image of the absorption band, confirming that, in this case, the emission is due to the nonaggregated dyes only.

On the other hand, the contribution of the H-dimers to the overall fluorescence spectrum is larger with the singly charged YOSAC1 and especially YOSAC3. Moreover, Table 1 reveals that the fluorescence quantum yields of these two dyes are noticeably larger. Because the overall fluorescence quantum yield is larger when the spectrum is dominated by the H-dimers, one can conclude that the intrinsic fluorescence quantum yield of the H-dimer is larger than that of the nonaggregated dye. This aspect is particularly important for the optimization of the fluorescence enhancement of DNA probes.[11]

By contrast to all nonaggregated dyes and H-dimers, the J-aggregates formed with YOSAC3 in buffered aqueous solutions are much more fluorescent. The J-aggregate fluorescence spectrum exhibits a narrow band centered at 540 nm and a broader band at 620 nm. The relative intensity of the latter was found to decrease as a function of time on the 10−15 min time scale. This effect was not further studied but is most probably due to a structural transformation of the aggregate. Because these J-aggregates do not fluoresce upon excitation in the absorption band of the nonaggregated dye, this emission has in principle no direct consequence on the use of YOSAC3 as a fluorescent DNA probe.

The fluorescence quantum yield of YOSAC1 was also measured in a few linear alcohols and was found to increase with increasing solvent viscosity, $\Phi_{fl}$ rising by a factor of 30 by going from MeOH to DeOH. Contrary to what was found in water, the fluorescence spectrum in these organic solvents is the mirror image of the absorption band.

Upon addition of DNA to aqueous buffer solutions, the fluorescence quantum yield of all four dyes strongly increases (Table 1), and their fluorescence spectrum becomes mirror image of their absorption spectrum (Figure 2C).

The fluorescence decay of the DNA-bound dyes in the nanosecond time scale could be well reproduced using biexponential functions. The resulting time constants, measured at the fluorescence maximum, are listed as $\tau_6$ and $\tau_7$ in Table 2. The relative amplitudes associated with $\tau_6$ and $\tau_7$ are on the order of 0.4 and 0.6, respectively, except for YOSAC1 for which they amount to 0.7 and 0.3. These time constants are very close to those reported for the corresponding YOYO dyes in DNA.[8,9] The presence of two decay components most probably reflects a distribution of lifetimes due to the heterogeneous base composition of salmon sperm DNA,[25,26] the fluorescence lifetime of YOYO-1 having been shown to depend on the base content.[8] The differences in the fluorescence quantum yields (Table 1) can be well accounted for by different average lifetimes of the dyes, pointing to a very similar radiative rate constant on the order of $k_{rad} = 1.3 \times 10^8\ s^{-1}$.

**TABLE 2: Time Constants Obtained from the Global Analysis of the Fluorescence Time Profiles of the Dyes, Free in Water and with DNA, Measured by FU ($\tau_1$−$\tau_5$) and TCSPC ($\tau_6$ and $\tau_7$)**

| dye | environment | $\tau_1$ (ps) | $\tau_2$ (ps) | $\tau_3$ (ps) | $\tau_4$ (ps) | $\tau_5$ (ps) | $\tau_6$ (ns) | $\tau_7$ (ns) |
|---|---|---|---|---|---|---|---|---|
| YO-PRO-1 | $H_2O$ | 0.17 | 0.22 | 1.3 | 3.1 | 28.7 | 2.6 | |
| YOSAC1 | $H_2O$ | 0.22 | 0.20 | 1.3 | 4.3 | 13.0 | 0.4 | 3.2 |
| YOSAC2 | $H_2O$ | 0.18 | 0.22 | 1.6 | 5.2 | 17.4 | 2.8 | |
| YOSAC3 | $H_2O$ | 0.18 | 0.27 | 2.2 | 8.0 | 48.7 | 0.9 | 3.2 |
| YO−PRO-1 | DNA | 0.20 | | 2.3 | | 40.8 | 1.9 | 4.1 |
| YOSAC1 | DNA | 0.18 | | 0.7 | | 29.7 | 2.2 | 4.8 |
| YOSAC2[a] | DNA | | | | | | 2.3 | 4.3 |
| YOSAC3[a] | DNA | | | | | | 2.5 | 4.5 |

[a] FU measurements with YOSAC2 and YOSAC3 in DNA were not performed.

TCSPC profiles measured with the free dyes in water are dominated (relative amplitude >0.99) by a decaying component that is too fast to be resolved with this technique. Nonetheless, two additional nanosecond components are required to reproduce the fluorescence decay of singly charged dyes, while a single nanosecond component is sufficient for doubly charged dyes (Table 2).

**Ultrafast Fluorescence Dynamics.** The ultrafast fluorescence dynamics of all free dyes in water and of YO-PRO-1 and YOSAC1 with different DNA concentrations was investigated by FU and was monitored at eight to nine different wavelengths spanning most of the fluorescence spectrum (480−630 nm) (Figure 3). At each DNA concentration, the time profiles were analyzed globally using eq 1c. The experimental data could not be properly reproduced with less than 2−4 exponentials in addition to the nanosecond components measured by TCSPC.

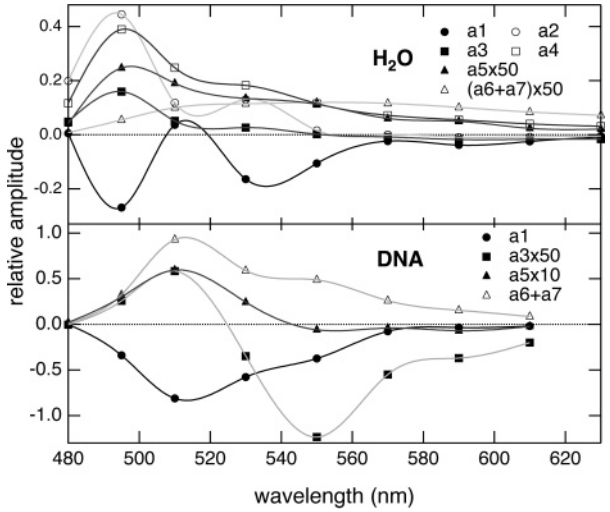


**Figure 4.** Wavelength dependence of the amplitude factors obtained from the global analysis of the fluorescence dynamics of YO-PRO-1 in water and with DNA (bp/dye ratio 12.3).

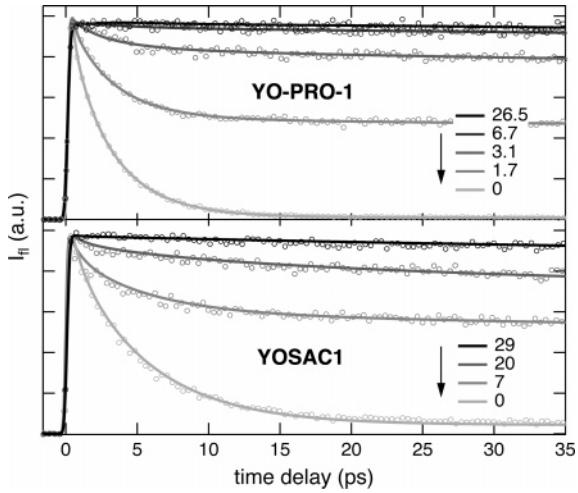


**Figure 5.** Bp/dye ratio dependence of the early fluorescence dynamics of YO-PRO-1 and YOSAC1.

A Gaussian function had to be included in the trial function to accurately describe the initial rise of the fluorescence intensity. Without this component, an unrealistically large IRF would have had to be assumed. The resulting time constants obtained with the free dyes and with YO-PRO-1 and YOSAC1 at high DNA concentration (bp/dye ratio of 12.3 for YO-PRO-1 and 29 for YOSAC1) are listed in Table 2. The spectral dependence of the amplitudes, $a_1-a_7$, associated with the various time constants is shown in Figure 4 for YO-PRO-1 free in water and with DNA. The sum of all positive amplitudes was normalized to one at 495 nm. The amplitudes at the other wavelengths were determined using eq 2. Because the steady-state spectra were recorded at lower concentrations than those used for the FU measurement, some underestimation of the relative amplitudes at long wavelengths cannot be ruled out. The decay-associated spectra obtained for the other dyes are qualitatively very similar to those found with YO-PRO-1.

In water, the amplitudes $a_1$ and $a_2$ have opposite sign at all wavelengths. The same feature was present with the other dyes and has also been reported for YOYO dyes.[9] In DNA however, no decaying component with a 200−300 fs time constant could be observed. The amplitude associated with $\tau_3$ is positive at short wavelengths and negative at long wavelengths in both water and DNA. This corresponds to a red shift of the fluorescence band and not to a decay of the excited-state population. The 3−8 ps component was not seen at high bp/dye ratio. Its relative amplitude, $a_4$, strongly depends on the DNA concentration and is the largest with the free dyes. Interestingly, the DNA concentration at which this component disappears depends on the dye, as illustrated in Figure 5. With the doubly charged YO-PRO-1, $a_4$ vanishes above a 6.7 bp/dye ratio, while a bp/dye ratio larger than 25 is required to suppress this component with the singly charged YOSAC1.

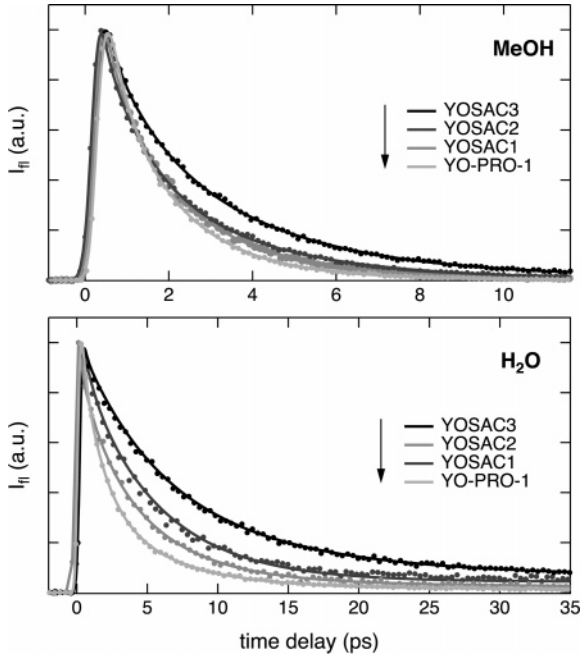


**Figure 6.** Fluorescence dynamics of the dyes in MeOH at 510 nm and in water at 550 nm.

**TABLE 3: Time Constants of the Dominant Fluorescence Decay Component of the Free Dyes in Solvents of Various Viscosity, $\eta$, at 20 °C**

| | | $\tau$ (ps) | | | |
|---|---|---|---|---|---|
| solvent | $\eta$ (cP) | YO-PRO-1 | YOSAC1 | YOSAC2 | YOSAC3 |
| $H_2O$ | 1.0 | 3.1 | 4.3 | 5.2 | 8.0 |
| MeOH | 0.55 | 1.6 | 1.9 | 2.5 | 3.5 |
| EtOH | 1.2 | 3.4 | 4.0 | | |
| BuOH | 2.95 | 9.6 | 13.1 | | |
| DeOH | 10.6 | | 28 | | |

The fluorescence dynamics at the band maximum was also measured with all dyes in MeOH and with YO-PRO-1 and YOSAC1 in a few longer-chained alcohols. The time profiles are dominated by a decay component that varies from 1.6 to 3.5 ps in MeOH and increases up to 28 ps in DeOH (Table 3). Figure 6 shows that in MeOH, the fluorescence intensity of all dyes decays to zero in less than 10−15 ps, while in water a long-lived component is present. The relative intensity of this component is larger with the singly charged dyes YOSAC1 and YOSAC3 than with the doubly charged dyes YO-PRO-1 and YOSAC2.

A weak component with a lifetime, $\tau_5$, on the order of 15−50 ps was found with all dyes, in both water and DNA. In water, its amplitude, $a_5$, is positive at all wavelengths, while in DNA it changes from positive to negative upon increasing wavelength.

To visualize the temporal evolution of the spectral shape of these dyes more easily, time-resolved emission spectra were reconstructed from the time profiles recorded at the different wavelengths. Such intensity-normalized spectra obtained with YO-PRO-1 in water and with DNA (bp/dye ratio 12.3) are

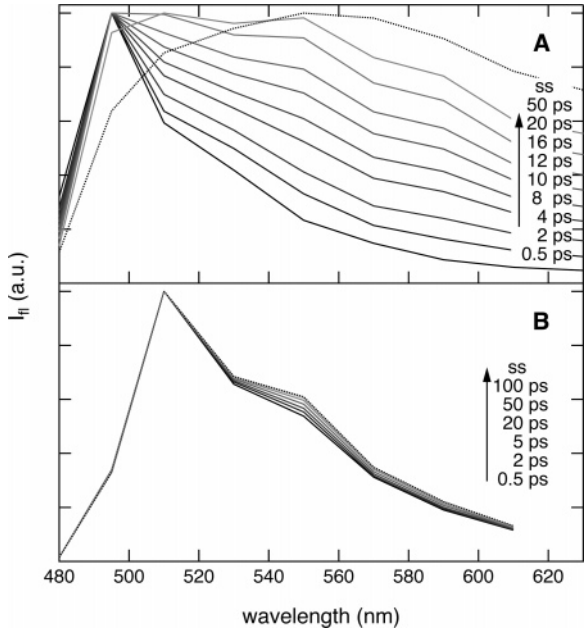


**Figure 7.** Intensity-normalized time-resolved fluorescence spectra of YO-PRO-1 in water (A) and with DNA (bp/dye ratio 12.3) (B) reconstructed using the time profiles recorded at different wavelengths, together with the steady-state (ss) spectrum.

illustrated in Figure 7. Although the number of wavelengths is small, it is immediately clear from this figure that the emission spectrum of free YO-PRO-1 exhibits fundamental changes, while only a weak broadening on the red side of the spectrum is observed with DNA-bound YO-PRO-1. The relatively small number of wavelengths used to reconstruct the spectra does not allow band shifts smaller than about 600 $cm^{-1}$ to be seen. Therefore, the red-side broadening of the spectrum of YO-PRO-1 with DNA should in fact correspond to a red shift of the whole band as suggested by the spectral dependence of $a_3$ and $a_4$ (Figure 4). Qualitatively similar time-resolved spectra are obtained with YOSAC1.

The fluorescence polarization anisotropy, $r$, measured with all free dyes in water was found to decay exponentially to zero with a time constant on the order of 25 ps. Because the average fluorescence lifetime of these free dyes is much smaller, the error on this time constant is very large (±8 ps). Figure 8 shows the decays of the fluorescence anisotropy measured with YO-PRO-1 and YOSAC1 at different bp/dye ratios. For both dyes, only a partial depolarization is observed, the residual anisotropy $r_\infty$ decreasing with increasing relative dye concentration. The time profiles of $r$ could be satisfactorily reproduced with a biexponential function with a time constant, $\tau_{r_1}$, on the order of 3−10 ps, and a second one, $\tau_{r_2}$, varying from 20 to about 200 ps. These time constants as well as their associated amplitudes are listed in Table 4. For both dyes, the residual anisotropy decreases with decreasing bp/dye ratio. However, the depolarization time constants obtained with YO-PRO-1 and YOSAC1 show opposite trends when going to small bp/dye ratio. In the case of YO-PRO-1, both $\tau_{r_1}$ and $\tau_{r_2}$ decrease weakly with decreasing bp/dye ratio. With YOSAC1 on the other hand, both time constants increase with decreasing bp/dye ratio. As discussed in more detail below, the anisotropy decay measured in the presence of DNA is due to the excitation energy hopping among the DNA-bound dyes and the difference in the effect of bp/dye ratio on the anisotropy time constant might reflect different binding modes.

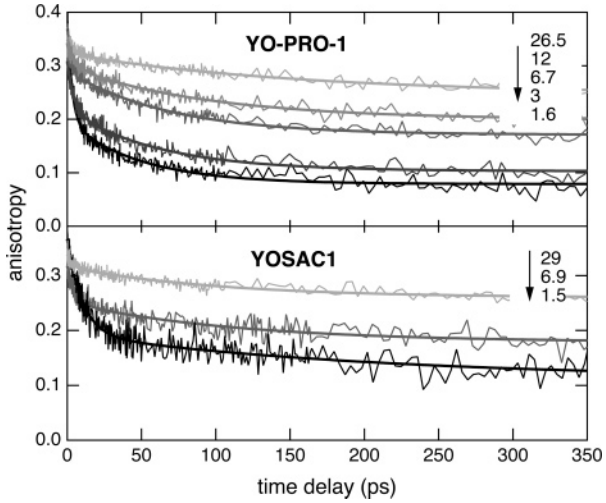


**Figure 8.** Bp/dye ratio dependence of the decay of the fluorescence polarization anisotropy of YO-PRO-1 and YOSAC1 at 510 nm.

**TABLE 4: Best-Fit Parameters Obtained from the Analysis of the Fluorescence Anisotropy Decay of YO-PRO-1 and YOSAC1 with DNA at Various bp/dye Ratios**

| bp/dye | $r_0$ | $r_1$ | $\tau_{r_1}$ (ps) | $r_2$ | $\tau_{r_2}$ (ps) | $r_\infty$ |
|---|---|---|---|---|---|---|
| | | | YO-PRO-1 | | | |
| 1.5 | 0.40 | 0.19 | 3.3 | 0.12 | 50 | 0.08 |
| 3 | 0.32 | 0.09 | 4.3 | 0.12 | 62 | 0.11 |
| 7 | 0.35 | 0.05 | 4.4 | 0.12 | 70 | 0.17 |
| 12 | 0.35 | 0.04 | 5.4 | 0.10 | 95 | 0.20 |
| 26 | 0.35 | 0.03 | 5.4 | 0.08 | 160 | 0.25 |
| | | | YOSAC1 | | | |
| 1.5 | 0.37 | 0.17 | 10 | 0.08 | 210 | 0.11 |
| 7 | 0.34 | 0.07 | 5.4 | 0.08 | 115 | 0.19 |
| 30 | 0.35 | 0.02 | 3.3 | 0.06 | 105 | 0.27 |

## Discussion

**Ultrafast Nonradiative Deactivation of the Free Dyes.** The dominant decay component observed with all free dyes in water can be unambiguously ascribed to nonradiative deactivation through large amplitude motion. First, the spectral dependence of the related amplitude, $a_4$, indicates that this process leads to a decay of the excited-state population and not to a spectral shift. Second, $a_4$ decreases with increasing bp/dye ratio and totally vanishes when all dyes are bound to DNA. Third, the time constant $\tau_4$ varies substantially with solvent viscosity. The viscosity dependence of the dynamics of processes associated with large amplitude motion, such as cis−trans isomerization, has been very intensively investigated both theoretically and experimentally.[27−32] The following empirical relationship has been proposed:[27]

$$\tau_{iso} \propto \eta^{\alpha} \qquad (3)$$

where $\tau_{iso}$ is the time constant of isomerization, $\eta$ is the solvent viscosity, and $\alpha$ is a factor that varies between 0.1 and 1, $\alpha = 1$ corresponding to the high friction limit in Kramers theory.[33] The value of $\alpha$ has been shown to be related to the barrier height for isomerization, the larger $\alpha$ values being observed with low barriers. This barrier height effect on the influence of viscosity on $\tau_{iso}$ has been rationalized by Grote and Hynes in terms of frequency-dependent friction.[34]

A doubly logarithmic plot of $\tau_4$ measured with YOSAC1 vs viscosity results in a straight line with a slope $\alpha$ of 1.0 ± 0.1. This indicates that the large amplitude motion responsible for

the nonradiative deactivation of this dye has no intrinsic barrier and is purely controlled by friction. This is in total agreement with the very short time constant found for this process. The small differences in $\tau_4$ measured with the various dyes are most probably due to volume variation of the groups involved in the large amplitude motion. Finally, it should be noted that the values found here with YO-PRO-1 and YOSAC2 are essentially the same as those measured with the corresponding YOYO compounds.[9]

**Aggregation.** The deviation of the fluorescence spectrum of the dyes from the mirror image of the absorption band and the concentration dependence of its shape clearly reveal that aggregation also plays a role in the fluorescence contrast mechanism of these monomeric dyes. However, this effect is much less important than with the YOYO dyes.[9] Indeed, contrary to these homodimeric compounds, the absorption spectrum of the YO dyes does not exhibit a very significant contribution of H-dimers. This is particularly true for the doubly charged YO-PRO-1 and YOSAC2 (see Figure 1). Moreover, the absorption spectrum of the YOYO dyes was found to dramatically change upon addition of DNA, because of the disruption of the intramolecular H-dimer upon intercalation. Such an effect is clearly not present with the YO dyes as testified by Figure 1D. Because the relative H-dimer concentration is very weak and because it is clearly observed in the fluorescence spectrum, one can conclude that the intrinsic fluorescence quantum yield of these dyes in water must be larger in the aggregated than in the nonaggregated form.

The H-dimers are most probably responsible for the slow fluorescence decay components measured in water. Indeed, the reconstructed fluorescence spectra of the free dyes after a few tens of ps are broad structureless and red-shifted relative to that of the nonaggregated dyes (Figure 7), in agreement with the spectrum of the amplitude associated with $\tau_6$ and $\tau_7$ (Figure 4). Moreover, as shown in Figure 6, this slow component is absent in organic solvents where aggregation is not operative. Furthermore in water, the amplitude of the slow component is larger with the singly charged than with the doubly charged dyes in agreement with the steady-state spectra that clearly show larger H-dimer contribution with singly charged compounds. The higher propensity of singly charged dyes to aggregate can be simply explained by a reduced electrostatic repulsion.

In the nonaggregated form, the dyes have a large radiative rate constant, $k_{rad}$, but a very short lifetime due to ultrafast nonradiative deactivation, hence their small fluorescence quantum yield. This deactivation channel is inhibited in the H-dimer and thus the excited-state lifetime of the latter is much longer. In principle, H-dimers are totally nonfluorescent because of the cancellation of the transition dipole moments in the lower excitonic state. However, if the two chromophores are not perfectly parallel in the aggregate, this cancellation is not complete, and thus the dipole moment for emission from the lowest excitonic state no longer vanishes. The $k_{rad}$ value of the H-dimer is thus not zero but is substantially smaller than that of the nonaggregated dye. As a consequence, the small contribution of the H-dimers to the total fluorescence in water is due to their small concentration as well as to their small fluorescence quantum yield.

**Origin of the Additional Decay Components.** The 150−200 fs Gaussian component with negative amplitude was seen with all dyes, both free in water and bound to DNA. This component was also required to reproduce the rise of the fluorescence intensity measured with the YOYO dyes.[9] The origin of this component is not totally understood. It might be due to the fact that the true instrument response function of the FU setup differs, because of group velocity dispersion or geometric effects, from that obtained from the cross-correlation of the pump and gate pulses or from Raman scattering. Similar problems have already been reported in the literature.[17] On the other side, because the FU experiments have been performed using 400 nm excitation, that is, with about 0.6 eV excess energy, intramolecular vibrational relaxation could also contribute to this delayed appearance of the fluorescence signal.[35]

By contrast, the short decay component with a time constant $\tau_2 \approx 200-300$ fs had only to be included to reproduce the fluorescence dynamics of the free dyes. The spectrum of the amplitude associated with this component is similar to the mirror image of the absorption spectrum, indicating that this component originates from the dye in the nonaggregated form. Above 580 nm, the amplitude is zero or very slightly negative. Because this decaying component has a lifetime very similar to that of the Gaussian rising component, the error on the amplitudes $a_1$ and $a_2$ should be quite large. A recent investigation of the excited-state dynamics of TO in MeOH has revealed the occurrence of a red shift and a broadening of the fluorescence band of this dye within the first 200 fs.[36] The authors have assigned this ultrafast spectral dynamics to an asymmetric distortion in the methine bridge during the relaxation of the excited molecule toward the global $S_1$ minimum. Considering the structural similarity of TO and the YO compounds, this process can also be expected to take place with the latter and to be at least partially responsible for the $\tau_2$ component. The decay-associated spectrum is not incompatible with such spectral dynamics. The instrument response function of the FU setup used here is however not short enough to properly resolve this process. The absence of this component with DNA-bound dyes supports this interpretation, the relatively rigid environment of the intercalated molecules preventing such distortion.

The component with the time constant $\tau_3 \approx 1-2$ ps can be related to a red shift of the fluorescence band as testified by its decay-associated spectrum where the sign of $a_3$ changes from positive to negative with increasing wavelength. The relative magnitude of $a_3$ at 495 nm, that is, at the blue side of the emission band, is on the order of 0.15 for all dyes in water. In DNA however, this value, measured with YO-PRO-1 and YOSAC1 only, is more than 5 times smaller. The time constant found for this component coincides very well with the time constant of diffusive solvation of bulk water.[37] Solvation in water has indeed been shown to be biphasic, with inertial motion taking place within a few tens of femtoseconds and diffusive motion in the 1 ps time scale. The location of the absorption and emission bands of the dyes depends on the environment as testified by the red shift of the spectra observed upon intercalation into DNA (Figures 1 and 2). Therefore, solvent relaxation should result in a dynamics Stokes shift of the fluorescence spectrum. However, a contribution to the Stokes shift from structural changes of the excited dyes in water, as reported for TO in MeOH,[36] cannot be ruled out. The smaller relative magnitude of $a_3$ in DNA could be explained by both a smaller exposure of the intercalated molecules to water and the rigid environment that restricts structural changes and thus suppresses this contribution to the Stokes shift.

Interestingly, a similar ~1 ps component has also been found with the YOYO dyes in DNA.[9] However, the relative amplitude of this component at 495 nm was on the order of 0.15−0.17, that is, much larger than that found here with YO-PRO-1 and YOSAC1. This large difference is possibly due to the effect of intercalation on the structure of the DNA helix. It has indeed

been shown that bisintercalation of YOYO-1 leads to a 106° unwinding of the DNA helix and to a helical repeat of 13 base pairs (instead of 10.4).[38] Such distortion is larger than that found with TOTO (60° unwinding) and is due to the constraint imposed by the relatively rigid structure of YOYO-1. Although no structural information exists, a smaller unwinding of the helix upon intercalation of YO dyes can be anticipated, since the structural constraint imposed by the linker is absent. Consequently, the exposure to water of YOYO dyes in the unwound DNA helix can be expected to be substantially larger than that of the YO dyes. This difference could thus account for the smaller relative contribution of the 1 ps Stokes shift observed here with the monomeric dyes in DNA compared with that found with their homodimeric equivalents.

However, the similarity of the $\tau_3$ value found in DNA with the diffusive solvation time of water might be coincidental, and this Stokes shift might in fact be due to structural relaxation of the DNA region around the excited intercalated dye, the smaller $a_3$ value with the YO dyes being possibly related to a different structural perturbation upon intercalation. The dynamic Stokes shift of a coumarin replacing a base pair in DNA has been recently shown to follow a power-law kinetics over six decades in times.[39] Moreover, no distinct component that could be assigned to bulk water was found. As a consequence, the origin of $\tau_3$ in DNA cannot be attributed unambiguously.

Although a component with a time constant $\tau_5 \approx 15-50$ ps was found with both free and DNA-bound dyes, the spectral dependence of the associated amplitude, $a_5$, is not the same for the free and DNA-bound cases, suggesting different origins. The spectral dependence of $a_5$ for free dyes is very similar to that of $a_4$ related to the ultrafast nonradiative deactivation. Moreover, $a_5$ is about 20 times smaller than $a_4$ pointing to a minor fraction of the excited-state population. Because of this small amplitude, the error on $\tau_5$ is large. We have no definitive explanation for this component. A slower nonradiative deactivation of molecules partially aggregated or adsorbed on the windows of the FU cell could account for it.

The spectral dependence of $a_5$ for the DNA-bound dyes suggests that $\tau_5$ corresponds to a red shift of the fluorescence. A red shift with a ~20 ps time constant has also been observed with a dye bound in the minor groove of DNA and has been ascribed to the motion of water molecules ordered at the DNA surface.[40,41] Because of their different binding mode, at least at high bp/dye ratio, the dyes investigated here should be less exposed to interfacial water molecules as already discussed above. Consequently, it is more reasonable to assign this red shift to structural dynamics of DNA. This time scale is also in agreement with that calculated for other biopolymers,[42] and is consistent with the conclusions of the above-mentioned study performed with a coumarin substituted for a base pair.[39] The time window and the spectral resolution of the FU measurements shown here are not sufficient to establish in detail the solvation dynamics of these intercalated dyes. This would however go far beyond the scope of this study.

**Decay of the Fluorescence Polarization Anisotropy.** The decay time of the polarization anisotropy of the free dyes in water is consistent with that of about 60 ps found with free YOYO-1. As discussed in detail for this dye in ref 9, this anisotropy decay can be unambiguously assigned to the reorientational motion of the molecule in water. On the other hand, reorientational motion can clearly not be invoked to account for the anisotropy decay of YO-PRO-1 and YOSAC1 in the presence of DNA. Table 4 and Figure 8 show that this anisotropy decay depends on the bp/dye ratio and that this dependence is not the same for YO-PRO-1 and YOSAC1.

By contrast, the decay of the anisotropy measured with YOYO-1 was found to be almost independent of the bp/dye ratio down to a ratio of about 10.[9] Above this value, the decay was found to be biphasic with 2.5−3 ps and 50−60 ps components of similar amplitude. Moreover, a residual anisotropy $r_\infty$ of 0.1 was measured. These findings were explained by excitation energy hopping (EH) between the two chromophoric moieties of YOYO-1, the dihedral angle between the two transition dipole moments being distributed around 83°. The smaller residual anisotropy measured at lower bp/dye ratios was attributed to the occurrence of intermolecular EH, namely, EH between different YOYO-1 molecules.

The anisotropy decays measured here with YO-PRO-1 and YOSAC1 with DNA can also be safely assigned to EH. However, the origin of the different bp/dye ratio dependencies is not so evident. The EH rate constant, $k_{EH}$, calculated within the framework of Förster theory is[43]

$$k_{EH} = 1.18V^2\Theta \tag{4}$$

where $k_{EH}$ is in $ps^{-1}$, $\Theta$ is the overlap integral between the donor emission and acceptor absorption spectra with the area normalized to unity on the $cm^{-1}$ scale, and $V$ is the dipole−dipole interaction energy in $cm^{-1}$. The latter is given by[44]

$$V = \frac{5.04|\mu|^2 f_L^{\,2}\kappa}{\epsilon_{op} d^3} \tag{5}$$

where $|\mu|$ is the magnitude of the transition dipole moment in D, $\kappa$ is the orientational factor, $d$ is the distance in nm, $f_L = (\epsilon_{op} + 2)/3$ is the Lorentz local field correction factor, and $\epsilon_{op}$ is the dielectric constant at optical frequencies, $\epsilon_{op} \approx n^2$, $n$ being the refractive index of the surrounding medium.

Both $|\mu|$ and $\Theta$ can be determined from the steady-state absorption and emission spectra.[44] The dipole moment for the $S_0-S_1$ transition amounts to 6.8 and 7.1 D for YO-PRO-1 and YOSAC1, respectively, while spectral overlap integrals of $8.1 \times 10^{-5}$ and $3.8 \times 10^{-5}$ were found. From eq 5 and assuming $n = 1.5$, the coupling energy between two parallel chromophores ($\kappa = 1$) at 1 nm is very similar for both YO-PRO-1 and YOSAC1 and amounts to 210 and 230 $cm^{-1}$, respectively. Inserting these values in eq 4 results in EH rate constants of 4.2 and 2.3 $ps^{-1}$. From these values, the depolarization of the fluorescence by EH is a priori not expected to differ very much for these two compounds. However, the geometrical parameters used for these calculations, namely, $d = 1$ nm and $\kappa = 1$, are not realistic for EH between DNA-intercalated dyes. The distance between two base pairs amounts to 0.34 nm,[45] and therefore, that between two intercalated chromophores, $i$ and $j$, can be approximately estimated as

$$d_{ij} = 1.02 \text{ nm} + n0.34 \text{ nm} \qquad n = 0, 1, 2, ... \tag{6}$$

The value of 1.02 nm originates from the fact that two intercalated dyes are separated by at least two base pairs.[46] Since no structural information on the DNA with intercalated dyes of the YO family exists, the distance between intercalated dyes is taken as being the same as the distance between two given base pairs. This is not totally realistic because the sugar backbone restricts the structural relaxation of the DNA helix upon intercalation. As a consequence, the distance between adjacent dyes, namely, two dyes without any additional intercalated dyes in between, should be smaller than that calculated from eq 6.

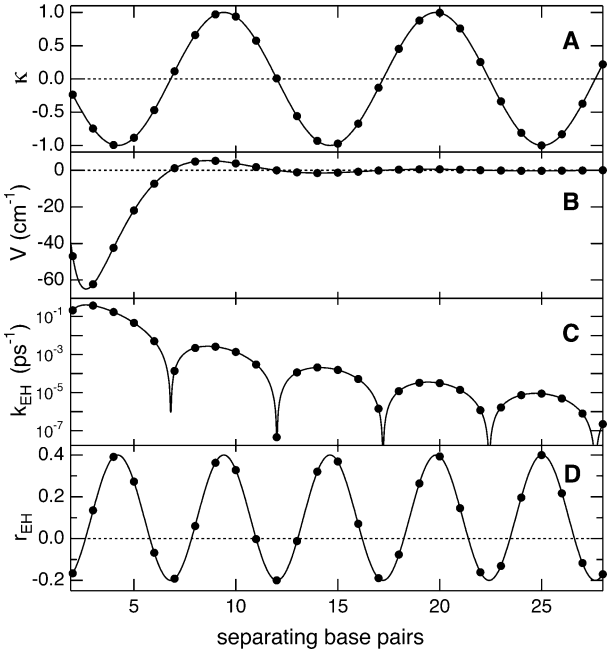


**Figure 9.** Effect of the distance, in units of separating base pairs, between two intercalated dyes on the orientational factor (A), the dipole−dipole interaction energy (B), the EH rate constant (C), and the fluorescence polarization anisotropy after a single EH step (D).

On the other hand, the distance between two nonadjacent dyes is most certainly larger than predicted by eq 6.

The orientational factor, $\kappa$, is totally controlled by the helicity of DNA, whose natural pitch in the B-form amounts to 3.54 nm.[45] Because of this, $\kappa$, calculated assuming that the dyes are coplanar, is larger for dyes separated by four base pairs ($\kappa^2 = 1$) than for dyes separated by only two base pairs ($\kappa^2 = 0.06$). As a consequence, the $d^{-6}$ dependence of the EH rate constant is strongly modulated by the periodicity of the orientational factor as illustrated in Figure 9. This figure also shows that EH is predicted to be faster for dyes separated by 3 than by 2 base pairs, the larger interchromophoric distance being compensated by a smaller angle between the transition dipoles. A similar modulation of the energy transfer efficiency has recently been reported by Lewis and co-workers.[47] Figure 9 also indicates that EH can be operative over a large number of base pairs, the EH efficiency amounting to 0.4 and to 0.1 with 14 and 20 base pairs, respectively.

The decay of the fluorescence polarization anisotropy via EH between the intercalated dyes is due to the helicity of DNA. Interestingly, orientational factors that favor EH are not those leading to a large depolarization. The loss of anisotropy upon a single EH process between two dyes separated by a varying number of base pairs is shown in Figure 9D.

To have a better insight into the effect of bp/dye ratio on the anisotropy decay, numerical simulations of the EH dynamics in a DNA helix with randomly intercalated dyes have been performed. In order to account for the variation of bp/dye ratio, the number of intercalated dye molecules was kept fixed at 12, while the number of base pairs was changed. These dyes were randomly substituted to a base pair, taking into account a minimum separation of two base pairs. For a given random arrangement, the 12 × 12 matrices of distance, orientational factor, and EH rate constant between each dye were determined. The initially excited dye was then chosen randomly, and the 12 equations of motion for the probability of each dye to be excited, $\partial P_i/\partial t$ , were then solved numerically. The time profile of the anisotropy was finally calculated as

$$r(t) = \sum_{i=1}^{12} P_i(t) r_{ij} \qquad (7)$$

where $r_{ij}$ is the polarization anisotropy for the case where the excitation has hopped on chromophore $i$ after having been initially on chromophore $j$. It is clear that the resulting $r(t)$ strongly depends on the arrangement of the dyes in the helix. As a consequence, this procedure was repeated for a large number of random arrangements, $N$, and an average anisotropy decay, $\langle r(t) \rangle$, was calculated. The value of $N$ was chosen so that the resulting $\langle r(t) \rangle$ was the same for each simulation, such outcome being realized with $N \geq 10^4$.

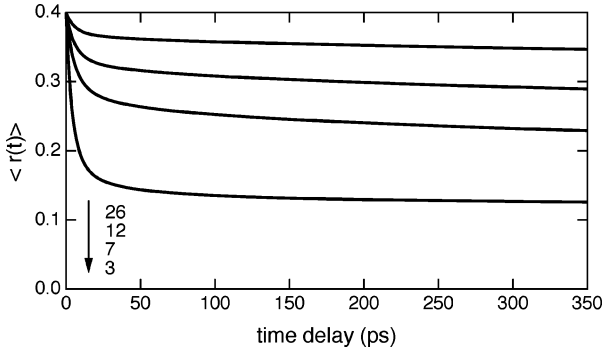


**Figure 10.** Simulated bp/dye ratio dependence of the decay of the fluorescence polarization anisotropy in DNA.

**TABLE 5: Best-Fit Parameters Obtained from the Analysis of the Simulated Decays of the Fluorescence Anisotropy in DNA ($r_0 = 0.4$)**

| bp/dye | $r_1$ | $\tau_{r_1}$ (ps) | $r_2$ | $\tau_{r_2}$ (ps) | $r_3$ | $\tau_{r_3}$ (ps) | $r_\infty$ |
|---|---|---|---|---|---|---|---|
| 3 | 0.19 | 4.2 | 0.06 | 16 | 0.02 | 125 | 0.13 |
| 7 | 0.07 | 4.6 | 0.06 | 15 | 0.06 | 400 | 0.21 |
| 12 | 0.06 | 5.6 | 0.02 | 25 | 0.05 | 370 | 0.27 |
| 26 | 0.03 | 5.7 | 0.01 | 25 | 0.03 | 430 | 0.33 |

The results of the simulations for various bp/dye ratios are depicted in Figure 10. The trend observed with the anisotropy decay of YO-PRO-1 is well reproduced. These calculated time profiles can be perfectly replicated with the sum of three exponential functions. To obtain a quantitative agreement with the experimental data, the coupling constants calculated using the parameters described above had to be multiplied by a correction factor of 0.6. The resulting best-fit parameters are listed in Table 5. One can see that the time constants, especially $\tau_{r_1}$, decrease weakly with decreasing bp/dye ratio, as observed experimentally. Moreover, the variations of the amplitude of the decaying components and of the residual anisotropy, $r_\infty$, are well reproduced. The small amplitude of the two slower components explains why only a single slow decay component could be detected in the experimental data.

This agreement between the simulations and the YO-PRO-1 data clearly supports the validity of the model used to describe the anisotropy decay, namely, EH between randomly intercalated dyes. This is a further evidence that the binding of YO-PRO-1 to DNA is completely noncooperative.[5,24]

The simulation without the correction factor of 0.6 results in too fast an anisotropy decay ($\tau_{r_1} \approx 1.9$ ps), indicating that EH is slower than predicted. The most probable origin of this difference is the structural change of DNA helix upon intercalation, which has been totally overlooked in the simulation. First, intercalation leads to an increase of the inter-base-pair distance

and therefore the actual interchromophoric distance differs from that calculated with eq 6. Second, intercalation of YOYO-1 has been shown to be accompanied by a 106° unwinding of the DNA helix and thus to an increase of the DNA pitch of about 30%.[38] Some local decrease of the helicity, although smaller than with YOYO-1, could also take place upon intercalation of a YO dye. According to our simulations, a 5% increase of the DNA pitch leads to an increase of $\tau_{r_1}$ from 1.9 to 2.4 ps. Third, the intercalated dyes have been assumed to be coplanar. Departure from coplanarity may lead to a reduction of the orientational factor and hence of the interaction energy, *V*.

The anisotropy decay measured with YOSAC1 at high bp/dye ratio can also be accounted for by EH between intercalated dyes. With the EH parameters for YOSAC1 discussed above, a $\tau_{r_1}$ value of 2.8 ps is obtained in the simulation, very close to the 3.3 ps found at high bp/dye ratio. However, the error on this time constant is large due to the very small associated amplitude ($r_1 = 0.02$), and this value should thus be considered with caution. A correction factor of 0.7 has to be used to reproduce the 5.4 ps value found at low bp/dye ratio. Lowering further the bp/dye ratio results in a slower anisotropy decay. This behavior differs from that found with YO-PRO-1 as well as that predicted by the simulations. At bp/dye ratios smaller than two, a significant part of the dye population cannot intercalate. The polarization anisotropy originating from these free dyes decays exponentially to zero by rotational diffusion with a time constant on the order of 25 ps (vide supra). A contribution of free dyes to the anisotropy could possibly explain the $r_\infty$ value of 0.08 measured with YO-PRO-1 at a bp/dye ratio of 1.5. Indeed, the residual anisotropy upon EH over chromophores in a coplanar arrangement but with a random distribution of dihedral angles between the transition dipoles moments should amount to 0.1. Nevertheless, a departure from coplanarity of the intercalated dyes could also account for the $r_\infty$ value of 0.08.

As shown in Figure 5, the fraction of free dyes at low bp/dye ratio should be significantly larger with the singly charged YOSAC1. Therefore, the contribution of the free dye population to the anisotropy decay should be larger than with YO-PRO-1. The measured 10 ps $\tau_{r_1}$-value could in fact be due to the contribution of two components around 5−6 and 25 ps that cannot be resolved because of the relatively small signal-to-noise ratio of the data.

An alternative explanation could be a different binding mode of YOSAC1 at high concentrations. Indeed, circular dichroism measurements have shown that at low bp/dye ratios, a second binding mode, most probably minor groove binding, was operative with both YO and YOYO dyes.[5] If both groove binding and intercalation take place with YOSAC1, the depolarization of the fluorescence by EH should follow a very different dynamics than that modeled assuming only intercalation. It is however not possible to simulate such a situation without knowing the exact position of the groove-bound dyes. Despite this, a slower depolarization of the fluorescence upon EH between groove-bound dyes is not unrealistic.

The fact that this anomalous behavior was observed with YOSAC1 and not with YO-PRO-1 might be due to their different structure and charge, both parameters being known to influence the binding properties of cyanines.[48−53]

## Conclusions

This investigation shows that despite very similar structures, the monomeric fluorescent DNA intercalators of the YO family exhibit substantial differences compared with their YOYO dimeric analogues. Indeed, the major fluorescence enhancement mechanism of the monomeric dyes upon intercalation is the inhibition of the large amplitude motion around the methine bridge that leads to an ultrafast nonradiative deactivation. Contrarily to the YOYO dyes, the disruption of nonfluorescent H-dimers upon binding plays only a minor role for the YO dyes, especially those with two positive charges. Moreover, some difference between YOYO and YO dyes, which could reflect a different distortion of the DNA helix upon intercalation, was observed.

This study also reveals that time-resolved fluorescence anisotropy combined with numerical simulations can be a very powerful tool for obtaining direct information on the binding mechanism of these dyes to DNA.

**Acknowledgment.** The authors wish to thank Prof. T. Deligeorgiev (Faculty of Chemistry, University of Sofia) for supplying the dyes. This work was supported by the Fonds National Suisse de la Recherche Scientifique through Project No. 200020-115942.

## References and Notes

(1) Selvin, P. *Science* **1992**, *257*, 885.
(2) Glazer, A. N.; Rye, H. S. *Nature* **1992**, *359*, 859.
(3) Rye, H. S.; Yue, S.; Wemmer, D. E.; Quesada, M. A.; Haugland, R. P.; Mathies, R. A.; Glazer, A. N. *Nucleic Acids Res.* **1992**, *20*, 2803.
(4) Armitage, B. A. *Top. Curr. Chem.* **2005**, *253*, 55.
(5) Larsson, A.; Carlsson, C.; Jonsson, M.; Albinsson, B. *J. Am. Chem. Soc.* **1994**, *116*, 8459.
(6) Mikelsons, L.; Carra, C.; Shaw, M.; Schweitzer, C.; Scaiano, J. C. *Photochem. Photobiol. Sci.* **2005**, *4*, 798.
(7) Carlsson, C.; Larsson, A.; Jonsson, M.; Albinsson, B.; Norden, B. *J. Phys. Chem.* **1994**, *98*, 10313.
(8) Netzel, T. L.; Nafisi, K.; Zhao, M.; Lenhard, J. R.; Johnson, I. *J. Phys. Chem.* **1995**, *99*, 17936.
(9) Fürstenberg, A.; Julliard, M. D.; Deligeorgiev, T. G.; Gadjev, N. I.; Vassilev, A. A.; Vauthey, E. *J. Am. Chem. Soc.* **2006**, *128*, 7661.
(10) Fürstenberg, A.; Julliard, M. D.; Deligeorgiev, T.; Gadjev, N.; Vassilev, A. A.; Vauthey, E. In *Femtochemistry VII: Fundamental Ultrafast Processes in Chemistry, Physics, and Biology*; Castleman, A. W., Jr., Kimble, M. L., Eds.; Elsevier: Amsterdam, 2006.
(11) Fürstenberg, A.; Deligeorgiev, T. G.; Gadjev, N. I.; Vasilev, A. A.; Vauthey, E. *Chem.—Eur. J.* **2007**, *13*, 8600.
(12) Deligeorgiev, T.; Gadjev, N.; Vasilev, A.; Drexhage, K.-H.; Yarmoluk, S. M. *Dyes Pigm.* **2006**, *70*, 185.
(13) Sambrook, J.; Fritsch, E. F.; Maniatis, T. *Molecular Cloning-A Laboratory Manual*, 2nd ed.; Cold Spring Harbor Laboratory Press: New York, 1989.
(14) Lakowicz, J. R. *Principles of Fluorescence Spectroscopy*, 2nd ed.; Kluwer Academic: New York, 1999.
(15) Morandeira, A.; Engeli, L.; Vauthey, E. *J. Phys. Chem. A* **2002**, *106*, 4833.
(16) Lang, B.; Angulo, G.; Vauthey, E. *J. Phys. Chem. A* **2006**, *110*, 7028.
(17) Horng, M. L.; Gardecki, J. A.; Papazyan, A.; Maroncelli, M. *J. Phys. Chem.* **1995**, *99*, 17311.
(18) Fürstenberg, A.; Vauthey, E. *Photochem. Photobiol. Sci.* **2005**, 260.
(19) Czikkely, V.; Forsterling, H. D.; Kuhn, H. *Chem. Phys. Lett.* **1970**, *6*, 207.
(20) Takahashi, D.; Oda, H.; Izumi, T.; Hirohashi, R. *Dyes Pigm.* **2005**, *66*, 1.
(21) Jelley, E. E. *Nature* **1936**, *138*, 1009.
(22) Scheibe, G. *Angew. Chem.* **1936**, *49*, 563.
(23) Iwasaki, M.; Higashinaka, K.; Tanaka, T. *J. Soc. Photogr. Sci. Technol. Jpn.* **1995**, *58*, 361.
(24) Petty, J. T.; Bordelon, J. A.; Robertson, M. E. *J. Phys. Chem. B* **2000**, *104*, 7221.
(25) Siemiarczuk, A.; Wagner, B. D.; Ware, W. R. *J. Phys. Chem.* **1990**, *94*, 1661.
(26) Verbeek, G.; Vaes, A.; Van der Auweraer, M.; De Schryver, F. C.; Geelen, C.; Terrell, D.; De Meutter, S. *Macromolecules* **1993**, *26*, 472.
(27) Velsko, S. P.; Fleming, G. R. *Chem. Phys.* **1982**, *65*, 59.
(28) Bagchi, B.; Oxtoby, D. W. *J. Chem. Phys.* **1983**, *78*, 2735.
(29) Akesson, E.; Sundström, V.; Gillbro, T. *Chem. Phys. Lett.* **1985**, *121*, 513.
(30) Zeglinski, D. M.; Waldeck, D. H. *J. Phys. Chem.* **1988**, *92*, 692.

(31) Sun, Y. P.; Saltiel, J. *J. Phys. Chem.* **1989**, *93*, 8310.
(32) Vauthey, E. *Chem. Phys.* **1995**, *196*, 569.
(33) Kramers, H. A. *Physica* (*Utrecht*) **1940**, *7*, 284.
(34) Grote, H. F.; Hynes, J. T. *J. Chem. Phys.* **1980**, *73*, 2715.
(35) Pigliucci, A.; Duvanel, G.; Lawson Daku, M. L.; Vauthey, E. *J. Phys. Chem. A* **2007**, *111*, 6135.
(36) Karunakaran, V.; Perez Lustres, J. L.; Zhao, L.; Ernsting, N. P.; Seitz, O. *J. Am. Chem. Soc.* **2006**, *128*, 2954.
(37) Jimenez, R.; Fleming, G. R.; Kumar, P. V.; Maroncelli, M. *Nature* **1994**, *369*, 471.
(38) Johansen, F.; Jacobsen, J. P. *J. Biomol. Struct. Dyn.* **1998**, *16*, 205.
(39) Andreatta, D.; Lustres, J. L. P.; Kovalenko, S. A.; Ernsting, N. P.; Murphy, C. J.; Coleman, R. S.; A., B. M. *J. Am. Chem. Soc.* **2005**, *127*, 7270.
(40) Pal, S. K.; Zhao, L.; Zewail, A. H. *Proc. Natl. Acad. Sci. U.S.A.* **2003**, *100*, 8113.
(41) Pal, S. K.; Zewail, A. H. *Chem. Rev.* **2004**, *104*, 2099.
(42) Nilsson, L.; Halle, B. *Proc. Natl. Acad. Sci. U.S.A.* **2005**, *102*, 13867.
(43) Pullerits, T.; Hess, S.; Herek, J. L.; Sundström, V. *J. Phys. Chem. B* **1997**, *101*, 10560.
(44) van Amerongen, H.; Valkunas, L.; van Grondelle, R. *Photosynthetic Excitons*; World Scientific: Singapore, 2000.
(45) Stryer, L. *Biochemistry*, 4th ed.; Freeman: New York, 1995.
(46) McGhee, J. D.; Von Hippel, P. H. *J. Mol. Biol.* **1974**, *86*, 469.
(47) Lewis, F. D.; Zhang, L.; Zuo, X. *J. Am. Chem. Soc.* **2005**, *127*, 10002.
(48) Bunkenborg, J.; Gadjev, N. I.; Deligeorgiev, T.; Jacobsen, J. P. *Bioconjugate Chem.* **2000**, *11*, 861.
(49) Mikheikin, A. L.; Zhuze, A. L.; Zasedatelev, A. S. *J. Biomol. Struct. Dyn.* **2000**, *18*, 59.
(50) Cao, R.; Venezia, C. F.; Armitage, B. A. *J. Biomol. Struct. Dyn.* **2001**, *18*, 844.
(51) Karlsson, H. J.; Eriksson, M.; Perzon, E.; Akerman, B.; Lincoln, P.; Westman, G. *Nucleic Acids Res.* **2003**, *31*, 6227.
(52) Sovenyhazy, K. M.; Bordelon, J. A.; Petty, J. T. *Nucleic Acids Res.* **2003**, *31*, 2561.
(53) Hannah, K. C.; Armitage, B. A. *Acc. Chem. Res.* **2004**, *37*, 845.